JACS
JOURNAL OF THE AMERICAN CHEMICAL SOCIETY

Communication

pubs.acs.org/JACS

Intrinsic Broad-Band White-Light Emission by a Tuned, Corrugated Metal–Organic Framework

Dorina F. Sava,[†] Lauren E. S. Rohwer,[‡] Mark A. Rodriguez,[§] and Tina M. Nenoff*[,†]

[†]Surface and Interface Sciences Department, [‡]Microsystems Integration Department, and [§]Materials Characterization Department, Sandia National Laboratories, Albuquerque, New Mexico 87185, United States

Supporting Information

ABSTRACT: Herein we report on the broad-band direct white-light originating from a single component emitter, namely a novel three-periodic metal–organic framework (MOF). This material features an unprecedented topology with (3,4)-connected nodes. The structure–function relationship in this system is driven by two complementary unique structural features: corrugation and interpenetration. Good correlation between simulated and experimental emission spectra has been attained, resulting in optimized color properties that approach requirements for solid-state lighting (SSL). Guided by the optimized calculated spectra, the tunability of the assembly was proven by the successful in-framework co-doping of Eu^{3+}. This resulted in significantly improved color properties, opening new paths for the rational design of alternative materials for SSL applications.

The ability to generate white light from a single phosphor is a highly sought alternative to existing approaches that achieve white light through color mixing. Current white LEDs for solid-state lighting (SSL) are based on blue InGaN LEDs that excite a yellow-emitting YAG:Ce phosphor.[1] The combination of blue and yellow light produces a cold white light that can be made warmer by combining the YAG:Ce with a red-emitting phosphor.[2] Warm white LEDs can also be achieved by combining the blue LED emission with red- and green-emitting phosphors.[3] There has been some interest in utilizing near-UV InGaN LEDs to excite blends of red-, green-, and blue-emitting phosphors to produce white LEDs. Unfortunately, the additional down-conversion step (near-UV to blue) significantly lowers the conversion efficiency of the device; additionally, it is difficult to find three phosphors that meet all of the criteria for SSL use.[4]

In this context, concerted efforts have been dedicated toward the discovery of novel materials for SSL. Metal–organic frameworks (MOFs) are a new class of solid-state materials with exceptional tunability and structural diversity. Traditionally, research into novel MOFs has focused on exploiting their highly accessible porosity and its applicability to gas storage and separations applications.[5] In recent years, the interest in these materials has been rationally extended to other challenging focus areas, such as photonics,[6] luminescence,[7] and SSL,[8] owing to (i) the intrinsic tunability and modularity of their highly ordered three-dimensional structures and (ii) their formation under mild synthesis conditions. White emission has only been observed in a small number of coordination compounds.[9] Of these, only a few emit white light directly,[9a−c] while others only exhibit white emission when excited at certain wavelengths[9d] or when rare-earth dopants (e.g., Dy^{3+}, Tb^{3+}, Eu^{3+}) are incorporated into the framework.[9e]

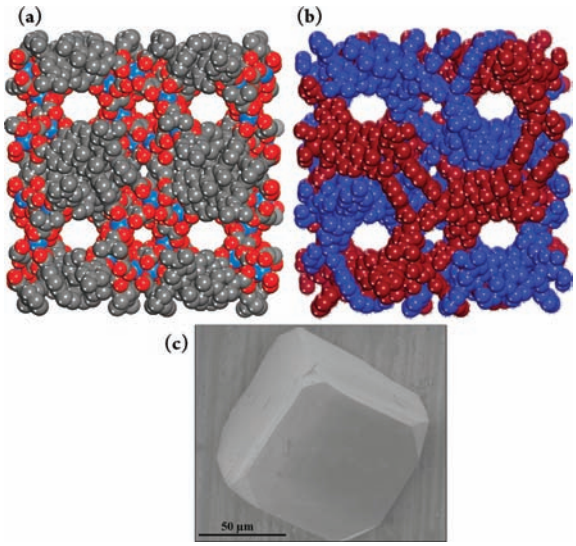

Figure 1. CPK[10] representations of (a) the X-ray single crystal structure; H-atoms have been omitted for clarity; atom color scheme: In = blue, C = gray, O = red; (b) view of 2-fold interpenetration in SMOF-1; (c) SEM image of SMOF-1 cubic single crystal.

In this study, we present a new MOF material featuring inherent broad-band direct white emission, with color properties that can be improved by incorporating red-emitting Eu^{3+} into the framework. We demonstrate the ability to tune the color rendering index (CRI), correlated color temperature (CCT), and chromaticity coordinates to approach the color properties required for SSL. The material forms by reacting $In(NO_3)\cdot H_2O$, 1,3,5-Tris(4-carboxyphenyl)benzene (BTB), and oxalic acid (OA) (1:1:1.5 molar ratio) in a *N,N′*-diethylformamide (DEF)/EtOH solvent mixture heated at 115 °C for 4 days, which produces crystals with polyhedral morphology, Figure 1; this represents the first extended framework constructed from BTB and In metal ions.

Received: November 30, 2011
Published: February 16, 2012

   dx.doi.org/10.1021/ja211230p | *J. Am. Chem. Soc.* 2012, 134, 3983–3986

The structure was determined by single crystal X-ray crystallography studies as $In(BTB)_{2/3}(OA)(DEF)_{3/2}$, also known as SMOF-1 (Sandia Metal−Organic Framework-1), Figure 1a. It crystallizes in the $Ia\bar{3}$ space group, has a cubic lattice with a large cell parameter, a = 33.975(3) Å, and is comprised of a doubly interpenetrated structure (Figure 1b). SMOF-1 has potential open channels in all directions, accessible through passages of ∼4.3 Å average dimensions, when considering the van der Waals radii of nearest atoms.

Further analysis of the guest-free SMOF-1 indicates the material's flexibility upon EtOH exchange and activation on the gas sorption analyzer Micromeritics ASAP 2020. This may be attributed to the length, as well as the torsion flexibility, of the BTB linker.[11] Single-crystal diffraction studies on the evacuated sample confirmed that the I-body centered cubic unit cell is maintained, but the cell parameter changes from 33.9750 to 31.8916 Å, which represents a significant volume adjustment of 6781 $Å^3$ (∼17.2% of initial cell volume). Similar breathing behaviors have been previously noted in other interpenetrated MOFs.[12] SMOF-1 is stable in common organic solvents and in water. Good agreement exists between the calculated and experimental powder X-ray diffraction (PXRD) patterns, verifying the purity of the as-synthesized sample (Figure S1).

Analysis of the crystal structure of SMOF-1 indicates the indium metal center adopts an eight-coordinate geometry, which is fully accommodated by two oxalates ligands in a bis(bidentate) fashion and by two BTB linkers, in two distinct ways: one BTB is binding the metal center in a bis(bidentate) mode, while the other binds in a monodentate fashion, resulting in a simplified node with tetrahedral geometry. The charge balance for the neutral framework is ensured by one protonated BTB linker.

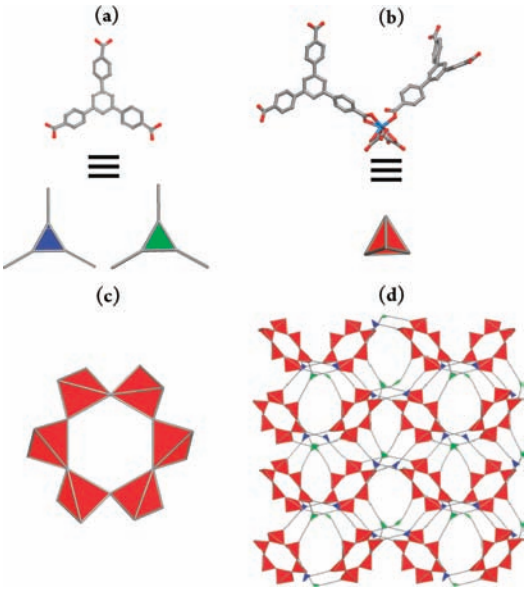

Figure 2. Molecular building blocks in SMOF-1, corresponding to (a) two topologically distinct 3-connected nodes and (b) a 4-connected node; (c) corner sharing tetrahedra forming a 6-member ring; and (d) topological representation of single net in SMOF-1.

There are two distinct 3-connected nodes in SMOF-1, which are defined by the BTB ligand connectivity (the extension point is chosen in the center of the BTB ligand, Figure 2a), while the 4-conntected node is defined by the metal center's points of extension, Figure 2b. The (3,4)-connected trinodal net reveals an unprecedented topology, not observed in any other material to date, Figure 1d; this was evaluated with the TOPOS software.[13] The short Schläfli (point) symbol for the net is $\{6^3.8^3\}3\{6^3\}2$, confirming the material's topological novelty. When considering a simplified alternative topological analysis, SMOF-1 can be interpreted as a (3,6)-connected net with pyrite topology (Figure S2). In this case, the 6-member ring corner sharing tetrahedra is viewed as a 6-connected node and the two corrugated BTB linkers within a distinct net are simplified to a fused 3-connected point of extension.

The photoluminescence (PL) properties of this material originate from the unique arrangement of the conjugated aromatic rings of the SMOF-1 framework (Figure S3). The overall connectivity of the In-based tetrahedrons forms 6-member ring arrangements, observed here for the first time in coordination compounds involving the BTB linker. In an individual net, the 6-member rings are further linked to each other in a corrugated fashion by two parallel symmetrically independent BTB linkers, with centroid−centroid distances between the central benzene rings of 4.727 Å (Figure S3). Interestingly, the struts within distinct nets are staggered, locating the middle of the rings' faces at a shorter distance of 3.574 Å from each other, thereby enabling aromatic π---π* stacking interactions (Figure S3).

PL excitation and emission spectra were collected on pristine SMOF-1. Excitation spectra were collected by scanning over UV wavelengths of 250−365 nm and monitoring at the 330 nm emission peak, Figure S4. Figure 3 highlights the measured

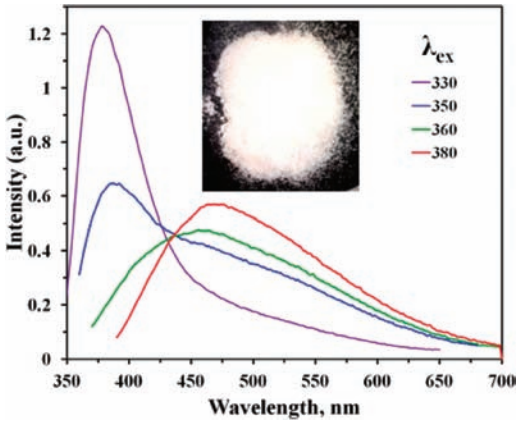

Figure 3. Emission spectra of SMOF-1, excited between 330 and 380 nm; inset: optical image of the white light emission in SMOF-1 powder sample excited at 365 nm.

emission when excited between 330 and 380 nm, with a maximum intensity around 390 nm, after exciting the sample at 330 nm. This peak coincides with a ligand-based emission and may be attributed to the cascade π---π* interactions occurring between the aromatic rings of the BTB linker. The additional broad-band emission observed when exciting the material between 350 and 380 nm can be further associated with the ligand-to-metal charge transfer (LMCT)BTB→M^{3+}transition.[14]

This results in overall direct white-light emission, which appears white to the eye. Assessment of the color properties for as-synthesized SMOF-1 revealed favorable CRI values that fall within intended ranges (81−85), but with very high CCT (21 642−33 290 K). Importantly, no changes to the color properties are noted on the guest-free SMOF-1.

dx.doi.org/10.1021/ja211230p | J. Am. Chem. Soc. 2012, 134, 3983−3986

In order to improve the intrinsic color properties of the pristine material, we introduced a narrow-band, red emission component into this system via Eu^{3+} doping. First, simulated spectra were generated by summing SMOF-1 and Eu^{3+} spectra, at excitation wavelengths of 350, 360, and 380 nm, respectively. Then, the amplitudes of each spectrum were varied to find the optimal color properties. The results of these simulations were then used to guide our experimental doping levels in SMOF-1.

Eu^{3+} was successfully doped at three concentrations into the SMOF-1 framework by the addition of a Eu metal source as a starting reagent; the eight-coordinated In site in SMOF-1 enables the introduction of large rare-earth ions like Eu. In a typical doping experiment, the amount of In was kept the same as that for the pristine SMOF-1, and additional Eu amounts equivalent to 2.5, 5, and 10% of the total mmol In concentration were included in the starting mixture. These are translated into actual 2.4, 4.8, and 9% total Eu partitioning with respect to In. However, for simplification of nomenclature, they are further referred to as 2.5, 5, and 10% Eu-doped SMOF-1. A maximum of 10% in-framework substitution of Eu for In was accomplished, as confirmed by SEM-EDS analyses (Figures S5, S6). Unit cell refinement of the 10% Eu-doped SMOF-1 sample reveals enlarged unit cell parameter dimensions of 34.57(6) Å, compared to 33.975(3) Å for the pristine sample, indicative of the in-framework substitution. Additionally, preliminary *in situ* temperature programmed XRD experiments on this sample indicate the formation of In_2O_3 and $EuInO_3$ phases (Figure S7); this finding may prove to be an attractive methodology for obtaining well dispersed lanthanide-based oxide mixtures.

PL spectra were collected for all three targeted concentrations of Eu-doped SMOF-1. Figure 4a shows a plot of calculated and experimental CCTs and CRIs for 2.5, 5, and 10% Eu-doped SMOF-1; the best values of CRI and CCT fall along or below the dashed line in the plot. The filled squares along this line correspond to the experimental values obtained from the 2.5, 5, and 10% Eu-doped SMOF-1 samples, excited at 350 nm. The experimental value that lies below the line corresponds to the 10% Eu-doped SMOF-1 sample excited at 394 nm.

By increasing the Eu^{3+} concentration to 10%, the CRI and CCT shifted closer to the set target of CRI ~90 and CCT ~3200 K.[15] The emission spectra of the 10% Eu sample excited between 330 and 394 nm are shown in Figure 4b. Several narrow-band emission peaks from Eu^{3+} are seen and are attributed to the parity forbidden ^5D-^7F transitions at ~590 nm (magnetic dipole transition $^5D_0$-$^7F_1$) and electric dipole transitions at ~616 nm ($^5D_0$-$^7F_2$), 650 nm ($^5D_0$-$^7F_3$), and 695 nm ($^5D_0$-$^7F_4$). The overall color properties of the 10% Eu-doped samples excited at different wavelengths are summarized in Table 1; additionally, a direct comparative analysis with pristine SMOF-1 is detailed in Table S2.

The Commission Internationale de l'Eclairage (CIE) has established optimum white-light chromaticity coordinates at (0.33, 0.33). When the 10% Eu-SMOF-1 sample is excited at 350, 360, 380, and 394 nm, the coordinates are (0.369, 0.301), (0.309, 0.298), (0.285, 0.309), and (0.304, 0.343), respectively, which closely approach targeted values (Figure 4b inset). Absolute quantum yield (QY) measurements were made by exciting the samples with diffuse light within an integrating sphere. The QY was found to be 4.3% when excited at 330 nm, which is modest as compared to traditional phosphors,[16] but falls within the expected range for similar reported systems.[9]

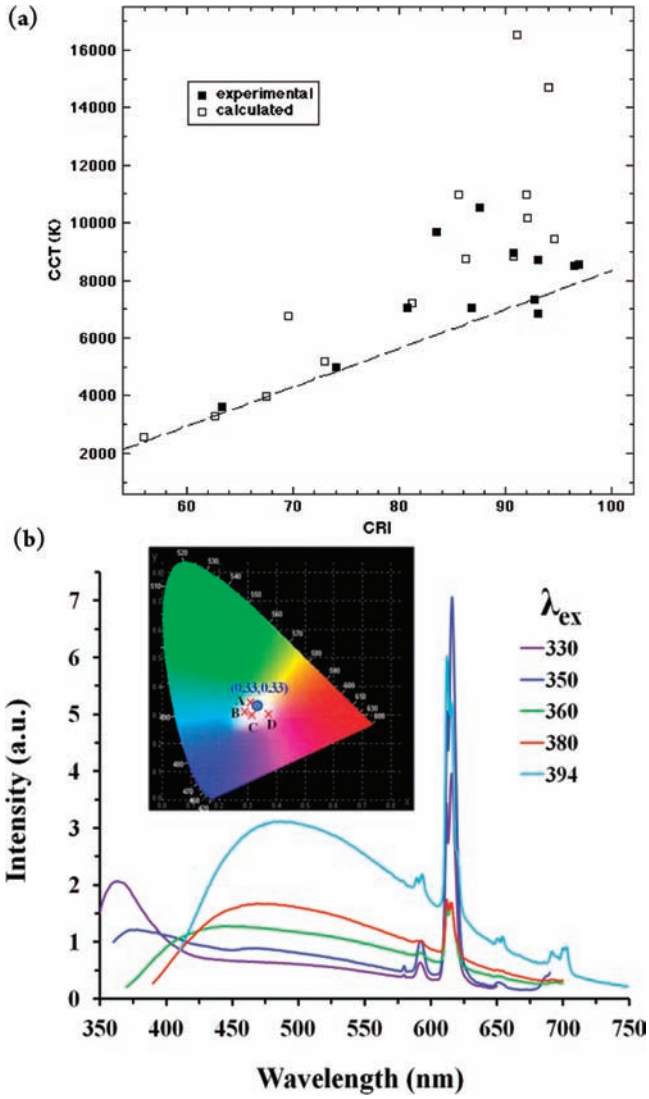

Figure 4. (a) Plot of calculated and experimental CCTs and CRIs for 2.5, 5, and 10% Eu-doped SMOF-1. (b) Emission spectra of 10% Eu-doped SMOF-1 when excited between 330 and 380 nm; inset: 1931 CIE chromaticity diagram highlighting corresponding chromaticity coordinates (A–D) approaching targeted values.

Table 1. Color Properties of 10% Eu-Doped SMOF-1 Sample

λ_{ex}	CRI	CCT (K)	*x*	*y*
350 (D)	63	3606	0.369	0.301
360 (C)	81	7068	0.309	0.298
380 (B)	93	8695	0.285	0.309
394 (A)	93	6839	0.304	0.343

The PL lifetime of the broad-band emission was measured by exciting the pristine, dried solid powder with a pulsed nitrogen laser at 337 nm, pumping a dye laser with the output set to 380 nm. Two silicon photodiode detectors with a response time of <1 ns were used, and the signals were averaged using a digital oscilloscope. The observed decay of the emission was slightly nonexponential, requiring the integration of the normalized decay curve to obtain the harmonic average lifetime,[17] which was 6.27 ns (Figure S8a). The PL lifetime of the 10% Eu-SMOF-1 emission was measured by exciting the doped powder with the pulsed nitrogen laser at 337 nm; two silicon

dx.doi.org/10.1021/ja211230p | J. Am. Chem. Soc. 2012, 134, 3983–3986

photodiode detectors were used. The decay was single exponential with a lifetime of 600 μs (Figure S8b). This long lifetime is due to the low oscillator strength of the 4f-4f transitions of Eu^{3+}.

To summarize, here we reported a novel MOF material featuring intrinsic broad-band direct white light emission. This prototype material represents a reliable tunable platform which allows for the significant enhancement of the associated color properties upon Eu^{3+} codoping, approaching values required for SSL applications. Improved efficiencies are currently being targeted on newly developed systems based on similar components.

■ ASSOCIATED CONTENT

Supporting Information

Details about sample preparation, XRD, TGA-MS, SEM-EDS, PL, and gas sorption measurements. This material is available free of charge via the Internet at http://pubs.acs.org.

■ AUTHOR INFORMATION

Corresponding Author

tmnenof@sandia.gov

Notes

The authors declare no competing financial interest.

■ ACKNOWLEDGMENTS

This work was supported by the U.S. DOE/NE/FCRD-SWG. Sandia National Laboratories is a multiprogram lab managed and operated by Sandia Corp., a wholly owned subsidiary of Lockheed Martin Corporation, for the U.S. DOE's NNSA under Contract DE-AC04-94AL85000.

■ REFERENCES

(1) Nakamura, S. *P. Soc. Photo-Opt. Ins.* **1997**, *3002*, 26.
(2) Mueller-Mach, R.; Mueller, G. O.; Krames, M. R.; Trottier, T. *IEEE J. Sel. Top Quant.* **2002**, *8*, 339.
(3) Mueller-Mach, R.; Mueller, G. O.; Krames, M. R.; Hoppe, H. A.; Stadler, F.; Schnick, W.; Juestel, T.; Schmidt, P. *Phys. Status Solidi A* **2005**, *202*, 1727.
(4) Phillips, J. M.; Coltrin, M. E.; Crawford, M. H.; Fischer, A. J.; Krames, M. R.; Mueller-Mach, R.; Mueller, G. O.; Ohno, Y.; Rohwer, L. E. S.; Simmons, J. A.; Tsao, J. Y. *Laser Photonics Rev.* **2007**, *1*, 307.
(5) (a) Zaworotko, M. J. *Nat. Chem.* **2009**, *1*, 267. (b) Rosi, N. L.; Eckert, J.; Eddaoudi, M.; Vodak, D. T.; Kim, J.; O'Keeffe, M.; Yaghi, O. M. *Science* **2003**, *300*, 1127. (c) Férey, G.; Serre, C.; Devic, T.; Maurin, G.; Jobic, H.; Llewellyn, P. L.; De Weireld, G.; Vimont, A.; Daturi, M.; Chang, J. S. *Chem. Soc. Rev.* **2011**, *40*, 550 and all references therein. (d) Li, J.-R.; Kuppler, R. J.; Zhou, H.-C. *Chem. Soc. Rev.* **2009**, *38*, 1477 and all references therein. (e) Sava, D. F.; Rodriguez, M. A.; Chapman, K. W.; Chupas, P. J.; Greathouse, J. A.; Crozier, P. S.; Nenoff, T. M. *J. Am. Chem. Soc.* **2011**, *133*, 12398. (f) Chapman, K. W.; Chupas, P. J.; Nenoff, T. M. *J. Am. Chem. Soc.* **2010**, *132*, 8897. (g) Chapman, K. W.; Sava, D. F.; Halder, G. J.; Chupas, P. J.; Nenoff, T. M. *J. Am. Chem. Soc.* **2011**, *133*, 18583.
(6) Wu, Y; Li, F.; Zhu, W.; Cui, J.; Tao, C.; Lin, C.; Hannam, P. M.; Li, G. *Angew. Chem., Int. Ed.* **2011**, *50*, 12518.
(7) Allendorf, M. D.; Bauer, C. A.; Bhakta, R. K.; Houk, R. J. T. *Chem. Soc. Rev.* **2009**, *38*, 1330 and all references therein.
(8) Furman, J. D.; Melot, B. C.; Teat, S. J.; Mikhailovsky, A. A; Cheetham, A. K. *Phys. Chem. Chem. Phys.* **2011**, *13*, 7622.
(9) (a) Liu, R.-S.; Drozd, V.; Bagkar, N.; Shen, C.-C.; Baginskiy, I.; Chen, C.-H.; Tan, C. H. *J. Electrochem. Soc.* **2008**, *155*, 71. (b) Wibowo, A. C.; Vaughn, S. A.; Smith, M. D.; zur Loye, H.-C. *Inorg. Chem.* **2010**, *49*, 11001. (c) Zhang, X. J.; Ballem, M. A.; Hu, Z. J.; Bergman, P.; Uvdal, K. *Angew. Chem., Int. Ed.* **2011**, *50*, 5728. (d) Wang, M.-S.; Guo, S.-P.; Li, Y.; Cai, L.-Z.; Zou, J.-P.; Xu, G.; Zhou, W.-W.; Zheng, F.-K.; Guo, G.-C. *J. Am. Chem. Soc.* **2009**, *131*, 13572. (e) Liu, K.; You, H.; Zheng, Y.; Jia, G.; Huang, Y.; Yang, M.; Song, Y.; Zhang, L.; Zhang, H. *Cryst. Growth Des.* **2010**, *10*, 16. (f) Liao, Y.-C.; Lin, C.-H.; Wang, S.-L. *J. Am. Chem. Soc.* **2005**, *127*, 9986. (g) Losilla, J. A.; Coutinho, D.; Balkus, K. J. *Microporous Mesoporous Mater.* **2008**, *113*, 325.
(10) Materials Studio v5.5.0.0 Accelrys; Accelrys Software Inc.: 2010.
(11) Chen, B.; Ma, S.; Hurtado, E. J.; Lobkovsky, E. B.; Liang, C.; Zhu, H.; Dai, S. *Inorg. Chem.* **2007**, *46*, 8705.
(12) (a) Chen, B. L.; Liang, C. D.; Yang, J.; Contreras, D. S.; Clancy, Y. L.; Lobkovsky, E. B.; Yaghi, O. M.; Dai, S. *Angew. Chem., Int. Ed.* **2006**, *45*, 1390. (b) Chen, B.; Ma, S.; Zapata, F.; Lobkovsky, E. B.; Yang, J. *Inorg. Chem.* **2006**, *45*, 5718.
(13) Blatov, V. A. *IUCr CompComm Newsletter* **2006**, *7*, 4.
(14) (a) Lin, Z.; Chen, L.; Yue, C.; Yan, C.; Jiang, F.; Hong, M. *Inorg. Chim. Acta* **2008**, *361*, 2821. (b) Guo, Z.; Li, Y.; Yuan, W; Zhu, X; Li, X; Cao, R. *Eur. J. Inorg. Chem.* **2008**, 1326.
(15) Department of Energy; Solid-State Lighting. http://www1.eere.energy.gov/buildings/ssl/.
(16) Chen, G.; Craven, M.; Kim, A.; Munkholm, A.; Watanabe, S.; Camras, M.; Götz, W.; Steranka, F. *Phys. Status Solidi A* **2008**, *205*, 1086.
(17) Martin, J. E.; Shea-Rohwer, L. E. *J. Lumin.* **2006**, *121*, 573.